Journal of Magnetic Resonance 201 (2009) 87–92

Contents lists available at ScienceDirect

Journal of Magnetic Resonance

journal homepage: www.elsevier.com/locate/jmr

A Modified Alderman–Grant Coil makes possible an efficient cross-coil probe for high field solid-state NMR of lossy biological samples

Christopher V. Grant [a], Yuan Yang [a], Mira Glibowicka [b], Chin H. Wu [a], Sang Ho Park [a], Charles M. Deber [b], Stanley J. Opella [a,*]

[a] Department of Chemistry and Biochemistry, University of California, San Diego, 9500 Gilman Drive, La Jolla, CA 92093-0307, USA
[b] Division of Molecular Structure and Function, Research Institute, Hospital for Sick Children, Toronto, Ont., Canada M5G 1X8

ARTICLE INFO

Article history:
Received 27 June 2009
Revised 10 August 2009
Available online 15 August 2009

Keywords:
Solid-state NMR
Probe
Sample heating
Alderman–Grant Coil
Membrane proteins

ABSTRACT

The design, construction, and performance of a cross-coil double-resonance probe for solid-state NMR experiments on lossy biological samples at high magnetic fields are described. The outer coil is a Modified Alderman–Grant Coil (MAGC) tuned to the ^{1}H frequency. The inner coil consists of a multi-turn solenoid coil that produces a B_1 field orthogonal to that of the outer coil. This results in a compact nested cross-coil pair with the inner solenoid coil tuned to the low frequency detection channel. This design has several advantages over multiple-tuned solenoid coil probes, since RF heating from the ^{1}H channel is substantially reduced, it can be tuned for samples with a wide range of dielectric constants, and the simplified circuit design and high inductance inner coil provides excellent sensitivity. The utility of this probe is demonstrated on two electrically lossy samples of membrane proteins in phospholipid bilayers (bicelles) that are particularly difficult for conventional NMR probes. The 72-residue polypeptide embedding the transmembrane helices 3 and 4 of the Cystic Fibrosis Transmembrane Conductance Regulator (CFTR) (residues 194–241) requires a high salt concentration in order to be successfully reconstituted in phospholipid bicelles. A second application is to paramagnetic relaxation enhancement applied to the membrane-bound form of Pf1 coat protein in phospholipid bicelles where the resistance to sample heating enables high duty cycle solid-state NMR experiments to be performed.

1. Introduction

There are two basic design strategies for probes for multiple-resonance NMR experiments. Either a single resonator, such as a solenoid coil, is tuned to two or three frequencies, or multiple resonators, each of which is tuned to one or two frequencies, are used. At high fields, the advantages of using a multiple resonator approach become more pronounced; these include the use of dedicated resonators optimized for their frequency of operation, and the reduction of complexity that results from physical isolation rather than relying solely on circuit elements, such as traps and filters, to provide electrical isolation of the frequencies. Furthermore, as magnetic field strengths increase, so do the differences in resonance frequencies between the low gamma nuclei (i.e. ^{15}N and ^{13}C) most commonly used in studies of proteins and ^{1}H. The frequency difference problem is most readily solved by the use of multiple resonators; an extreme example is Electron Paramagnetic Resonance (EPR) probes designed to perform Electron Nuclear Double Resonance (ENDOR) experiments where there is no choice but to use individual resonators optimized for the gigahertz electron resonance and the megahertz nuclear resonances frequencies [1]. The drawbacks of multiple resonator probes are chiefly geometric, with one or more of the resonators sacrificing filling factor in nested arrangements.

The most commonly implemented probe design for solid-state NMR consists of a single resonator (typically a solenoid coil) double- or triple-tuned with a Cross-Waugh type of circuit [2–4] or a variation that employs transmission lines [5,6]. In these probes a solenoid coil with between 4 and 7 turns is typically employed because its inductance represents a good compromise: high enough for low frequency operation (e.g. 70.9 MHz ^{15}N at 16.4 T) and low enough so that the resonator can be effectively tuned to the much higher ^{1}H resonance frequency (e.g. 700 MHz for ^{1}H at 16.4 T). As magnetic field strength increases this inductance trade-off becomes more problematic with the disparate frequencies placing opposing demands on the inductance of the coil.

For the study of proteins and other biopolymers by solid-state NMR there are two additional factors to be considered. The first is the high dielectric strength of the samples, which typically

* Corresponding author. Address: Department of Chemistry and Biochemistry, University of California, San Diego, 9500 Gilman Drive, Natural Sciences Building, Rm. 3121, La Jolla, CA 92093-0307, USA. Fax: +1 858 822 4821.
E-mail address: sopella@ucsd.edu (S.J. Opella).

1090-7807/$ - see front matter © 2009 Elsevier Inc. All rights reserved.
doi:10.1016/j.jmr.2009.08.009

contain large amounts of water and salts. These electrically lossy samples can significantly reduce the probe Q (quality) factor and shift the tuned frequency down substantially, resulting in a loss of probe efficiency and a circuit design challenge to accommodate a large tuning range. In addition, lossy biological samples are very efficiently heated during RF irradiation [7–9]. Several technologies have emerged in recent probe designs, each seeking to prevent the undesired and deleterious sample heating that originates from the conservative electric fields generated by the multiple-tuned resonator. For example, the scroll coil has a reduced electric field at the sample and a relatively low inductance resulting in a reduction in sample heating [10,11]. Other types of resonators can also be employed to reduce RF heating by minimizing the conservative electric fields within the sample volume [12,13]. Recently, we have described an approach based on the principles of a Faraday shield, the strip-shield insert, that localizes the undesirable electric fields outside of the sample volume, effectively shielding the sample from the heating effects of a solenoid coil [14].

An alternative approach is to use a low inductance resonator at the ^{1}H frequency while employing a solenoid coil for the low frequency channels in a cross-coil configuration [15–18]. Here, we describe a cross-coil double-resonance probe using two singly tuned resonators, a Modified Alderman–Grant Coil (MAGC) tuned to the ^{1}H frequency and a solenoid coil tuned to the low gamma ^{15}N frequency. These two resonators are nested to form a compact cross-coil pair. The low inductance MAGC is on the outside, and due to its low inductance and relatively small filling factor, it minimizes the effects of RF heating, Q damping, and frequency shift induced by the presence of a lossy sample. The inner coil is a multi-turn solenoid optimized for low frequency operation. This probe has a more compact resonator geometry then previously described examples of cross-coil probes [16–18] and a different circuit topology.

2. Results

The MAGC [19,20] shown in Fig. 1 is machined from a solid rod of oxygen free copper. The geometry of this coil has been optimized to create a homogenous B_1 field in the central region, which is occupied by the 5 mm ID multi-turn inner solenoid coil in the completed probe shown in Fig. 2. The MAGC in Fig. 1 has a thickness of 0.5 mm, an ID of 9 mm, a total length of 1.5 cm, and a window length (bottom gap) of 10.25 mm. The window occupies 280° of the coil. Three parallel strings of four ATC chip capacitors in series bridge the window (bottom gap) of the MAGC. The 0.5 mm slot (top gap) that runs the entire length of the coil reduces unwanted

Fig. 1. The Modified Alderman–Grant Coil (MAGC). Three parallel strings of four series ceramic chip capacitors can be seen in the 10.25 mm bottom gap of a 9 mm ID MAGC coil of 0.5 mm thick oxygen free copper. A top gap of 0.5 mm running the length of the long axis of the MAGC is located in the top portion of the coil.

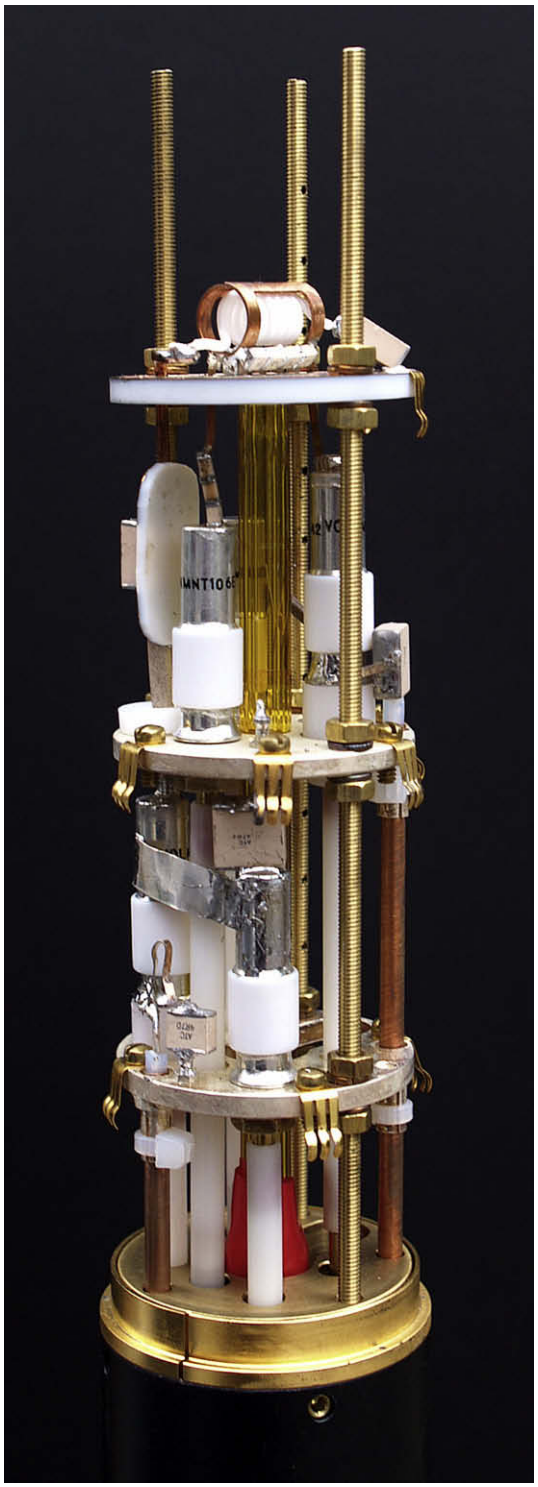

Fig. 2. Photograph of the completed circuit assembly in the NMR probe head. The MAGC and inner coil of white Teflon coated wire resides at the top most level.

inductance along the long axis of the MAGC. With the capacitors in place, the resulting assembly produces a B_1 field orthogonal to the long axis of the MAGC, through the window [19,20]. The inner solenoid coil produces a B_1 along the long axis of the solenoid/MAGC pair. As such, the resonators are in a cross-coil configuration (Fig. 2) with orthogonal B_1 fields that minimize inductive coupling and RF interference.

The resonance frequency of the MAGC is determined by the total capacitance in the bottom gap. In this example, the MAGC alone resonates at approximately 800 MHz with 3.7 pF capacitance in the bottom gap ($C7^*$ in Fig. 3). The final frequency is reduced when incorporated into the probe circuit by the effects of the coil leads, stray inductance in the total circuit, and stray capacitance between the outer MAGC and the inner solenoid coil. The relatively low inductance of the MAGC ensures a concomitantly small voltage drop across the coil, and a relatively high current flow through the circuit, requiring attention to the choice of capacitors, particularly those at position $C7^*$. The high current nature of the circuit led to the use of the smaller B case ceramic chip capacitors from American Technical Ceramics (www.atceramics.com), which we have found to be much more effective at dissipating heat than the larger E case ATC capacitors that are more commonly used in solid-state NMR probes because of their voltage handling capabilities.

The ^{1}H circuit diagrammed in Fig. 3 has been tested extensively and, when properly implemented, is reliable and electrically well behaved at RF powers up to 350 W. The variable capacitor C2 adjusts the match, and the variable capacitor C11 tunes the circuit. The variable capacitor C3 is used to balance the circuit. All of variable capacitors are from Voltronics Corporation (www.voltronicscorp.com). The final probe assembly with a 48 mm OD is pictured in Fig. 2. Variable temperature control is accomplished as previously described [10].

It is essential to balance [21] the circuit in order for the MAGC to exhibit optimal efficiency, homogeneity, and power handling capabilities. Because it is difficult to theoretically determine the correct value of the balance capacitor, we balance the circuit empirically; the capacitance of C3 is adjusted while monitoring the B_1 homogeneity and nutation frequency. Following this procedure RF homogeneity of 86%, the ratio of the amplitude of the nutation curve following an 810° pulse to that of a 90° pulse expressed as a percentage, is measured for a typical 160 µl bicelle sample in a 5 mm flat bottom NMR tube filled to an approximate depth of 10 mm. The ^{1}H resonance nutation plot is shown in Fig. 4, and the performance and homogeneity data are summarized in Table 1.

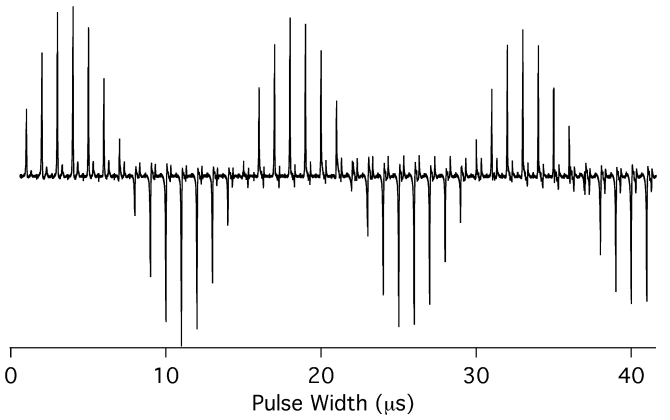

Fig. 4. ^{1}H resonance nutation plot for a 160 uL sample in 5 mm flat bottom NMR tube. The observed ^{1}H NMR signals from H_2O in the sample are plotted as a function of pulse duration in microseconds.

Table 1
Summary of probe performance.

Channel	Nutation frequency, power	Homogeneity (A_{810}/A_{90}) × 100%
^{1}H	67 kHz, 250 W	86%
^{15}N	50 kHz, 350 W	80%

It should be possible to replace the variable capacitor C3 with a fixed capacitor of the determined value, and this would free up valuable space for additional circuit elements in triple-resonance implementations of this basic design.

The inner coil is approximately seven turns, with an inner diameter of 5 mm, wound from 20 AWG round wire (Alpha Wire Company, www.alphawire.com) with a PTFE (polytetrafluoroethylene) coating of 0.25 mm, which serves as an insulating dielectric layer between the inner and outer coils to prevent arcing between the coils. The inner coil is driven by a standard tuning circuit in a configuration that is balanced by the appropriate choice of capacitor C17. Circuits without capacitor C17 are approximately 5% more efficient; however, having a capacitor in this position is essential to achieve good ^{1}H frequency to ^{15}N frequency isolation across a broad range of values of the trim capacitors C13 and C15. As a result, the value of C17 is optimized for its isolation effects rather than strictly as means of electrically balancing the inner coil with regard to the ^{15}N voltage.

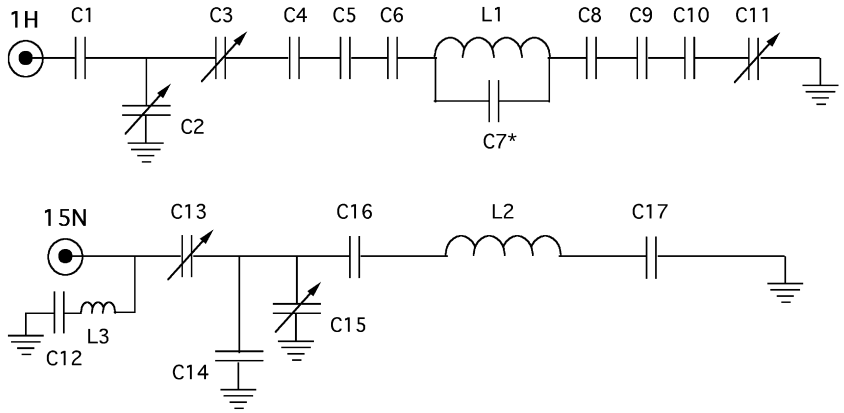

Fig. 3. Circuit diagram for the probe shown in Fig. 2. L1 represents the MAGC and L2 is the seven turn 5 mm inner solenoid coil. The values of the capacitors are: C1 = 2.2 pF, C4 = 6.8 pF, C5 = 6.8 pF, C6 = 6.8 pF, C8 = 6.8 pF, C9 = 6.8 pF, C10 = 6.8 pF, C12 = 4.7 pF, C14 = 47 pF, C16 = 120 pF, C17 = 120 pF. The capacitance $C7^*$ is 3.7 pF total integrated into the MAGC (Fig. 1) and consists of three parallel strings of four series ceramic chip capacitors. Capacitors C2, C3, C11, C13, and C15 are variable capacitors with a range of 1–10 pF.

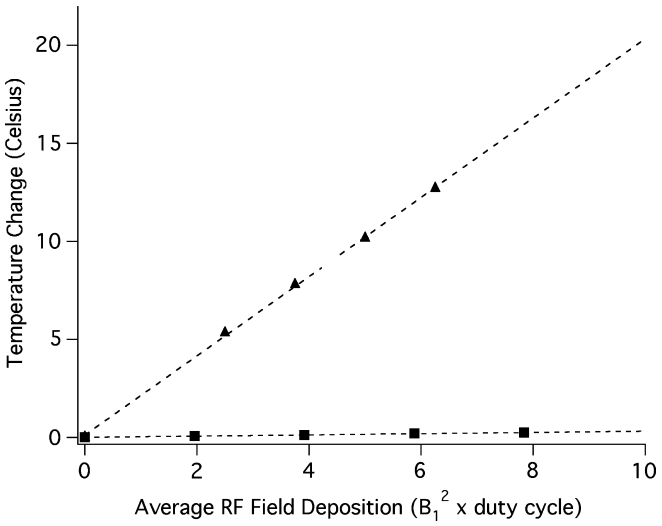

Fig. 5. Sample temperatures measured by chemical shifts plotted as a function of the average RF field deposition, a B_1 field of 50 kHz was used. The dashed lines are linear fits to the experimental data with slopes of 0.032 (°C/kHz^2) for the 699.9 MHz ^{1}H irradiation (squares) and 2.02 (°C/kHz^2) for the 70.9 MHz ^{15}N irradiation (triangles). ^{1}H B_1 fields were measured directly using the heating sample, ^{15}N B_1 fields were determined indirectly using a bicelle sample.

The RF heating effects have been measured as previously described [10,11]. We assessed sample heating by monitoring the ^{1}H chemical shift of the H6 resonance of Na_5[TmDOTP] (Macrocyclics, www.macrocyclics.com), the sodium salt of the complex between the thulium ion and the macrocyclic chelate 1,4,7,10-tetraazacyclodecane-1,4,7,10-tetrakis(methylene phosphonate) [22]. The Na_5[TmDOTP] sample included an additional 70 mM of NaCl so that its dielectric properties are comparable to the "worst-case" lossy aqueous samples that we study, such as protein-containing phospholipid bilayers [10]. The Na_5[TmDOTP] containing test sample, was loaded into a 5 mm sample tube to a depth of approximately 10 mm, which corresponds to a volume of 160 µl. The RF induced heating was measured for both the ^{1}H channel (700 MHz) and the ^{15}N channel (70.9 MHz) using the pulse sequence described previously [10]. In both cases, the sample temperature following RF heating is monitored using the chemical shift of H6 of Na_5[TmDOTP]. Fig. 5 illustrates the heating effects at both the ^{15}N and ^{1}H frequencies by plotting the sample temperature change (°C) as a function of the B_1 field deposition, which is the product of the square of the B_1 field and the duty cycle. Typical solid-state NMR experiments on stationary lossy samples are in the range of 4–10 RF field deposition for ^{1}H irradiation. Thus, the ^{1}H channel is expected to elevate the sample temperature by no more then 0.4 °C under the same experimental conditions where a conventional double tuned solenoid coil probe would elevate the sample temperature by 10 °C. RF irradiation through the inner coil results in a small, but non-negligible heating at the ^{15}N frequency of 70.9 MHz, a consequence of using a high inductance solenoid coil. Typical solid-state NMR experiments on lossy samples are in the range of 1–2 average RF field deposition for ^{15}N irradiation. Thus, it is expected that the probe described here will elevate the sample temperature by less than 4 °C during typical experiments.

NMR studies of domains of the Cystic Fibrosis Transmembrane Conductance Regulator (CFTR) in phospholipid bilayers are very challenging because of the sample heating that occurs with these lossy samples. The initial samples containing the TM3/4 V232D segment of CFTR would form ordered and well-aligned bicelles only at low concentrations, near the threshold of solid-state NMR detection. Increasing the protein concentration resulted in precipitated protein and ^{15}N NMR powder pattern line shapes in the spectra. Typically, salt concentrations are minimized in sample preparations due to the deleterious effects that solvated ions have on NMR probe performance and because of the RF heating that is enhanced by the conductivity of the sample [19,23]. However, it was found that CFTR would reconstitute successfully in $q = 3.2$ bicelles only in the presence of an electrically significant amount of added salt. The final sample preparations contain 50 mM NaCl. The spectrum displayed in Fig. 6A is consistent with a well-aligned membrane protein that has a significant fraction of its residues in transmembrane helices. This illustrates the value of this probe design for dealing with tuning changes induced by lossy samples.

In a second example, the membrane-bound form of Pf1 coat protein in similar $q = 3.2$ bicelles was studied with the addition of 20 mM Cu–EDTA to the solution to reduce the value of ^{1}H T_1 and hence the duration of the recycle delay required for the experiments [24,25]. By using a 1.5 s recycle delay, we were able to obtain a two-dimensional spectrum (Fig. 6B) in one-fourth the time previously needed. Notably, no significant line broadening is observed due to sample heating when it is compared to the spectrum obtained with a recycle delay of 6 s.

3. Discussion

The MAGC in a cross-coil probe offers several advantages over conventional designs that utilize a double- or triple-tuned solenoid

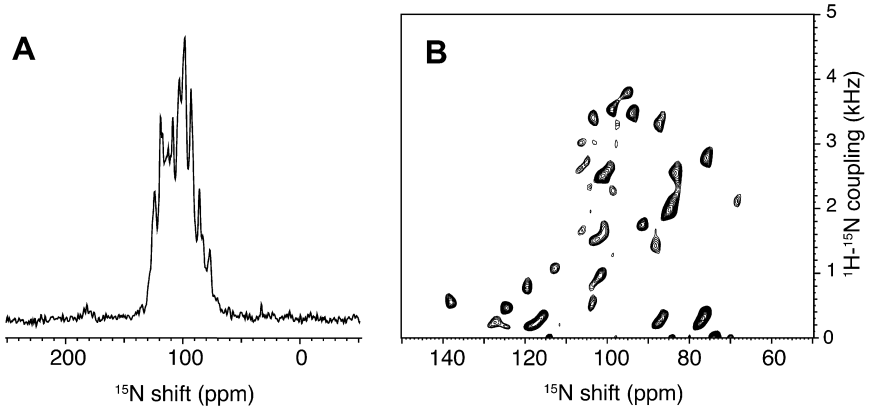

Fig. 6. Experimental NMR spectra of lossy biological bicelle samples aligned magnetically with their normals perpendicular to the magnetic field using the cross-coil solid-state MAGC NMR probe. (A) One-dimensional ^{15}N chemical shift spectrum of uniformly ^{15}N-labeled CFTR TM3/4 V232D. (B) Two-dimensional ^{15}N–^{1}H separated local field spectrum of uniformly ^{15}N-labeled Pf1 major coat protein. The ^{15}N and ^{1}H average RF field depositions (kHz^2) are 0.4 and 4.6 for (A) and 5.2 and 11 for (B).

coil. The low inductance outer ^{1}H MAGC coil is very effective at reducing RF heating. The simple tuning circuit utilizes a minimum number of tuning elements for the inner coil and provides freedom to choose an inner coil of optimal inductance for the low frequency detection channel. This contributes to good sensitivity in direct detection experiments. This implementation offers potential advantages compared to other cross-coil low-E probes. The outer MAGC is relatively compact, which improves the performance of the ^{1}H channel, and results in a compact overall resonator structure that fits inside narrow bore magnets. The main disadvantage of this design results from the very same properties of the MAGC resonator that minimize the RF heating, namely the low inductance of the MAGC and its relatively low filling factor, which would render the coil rather insensitive for direct observation of ^{1}H signals. For ^{1}H-detection, the design could be reversed, placing the MAGC coil on the inside and the low frequency solenoid coil on the outside of a nested cross-coil pair.

Taken together, the advantages resulting from the compact cross-coil design and the optimization of the respective high and low frequency coils enables the study of lossy biological samples and the use of high duty cycles in solid-state NMR experiments that require high RF power irradiations in high field magnets.

4. Experimental

4.1. Expression and purification

The ^{15}N labeled form of the CFTR TM3/4 V232D helical hairpin construct was expressed and purified as previously described [26–28]. In each of these constructs, wild type Cys225 was changed to an Ala to avoid disulfide bond formation between different helical hairpin molecules. cDNA encoding for residues 194–241 (TM segments 3 and 4, with the mutation at position 232) of CFTR was subcloned into PET-32a. This construct also contains a fusion protein (thioredoxin) to aid in solubilizing the hydrophobic CFTR fragment, an S-tag for detection by Western blots, and a His-tag for purification purposes. In the construct employed in the present work, the S-tag from the vector (KETAAAKFERQHMDS) was removed by using Stratagene's QuikChange site-directed mutagenesis kit for which forward (GGTTCTGGTATGCCAGATCTGGGTACC) and reverse (GGTACCCAGATCTGGCATACCAGAACC) primers were designed. The resulting constructs were transformed into BL-21 cells in M9 medium (M9 salts: 0.8% Na_2HPO_4 (w/v), 0.4% KH_2PO_4 (w/v), 0.05% NaCl (w/v), and 0.1% $^{15}NH_4Cl$ (purchased from Cambridge Isotope Laboratories) in 1 L water, pH adjusted to 7.5). Prior to cell growth, the medium was supplemented with biotin and thiamine (1 mg/L of each); sterile $MgSO_4$ and $CaCl_2$ stock solutions to final concentrations of 1 mM and 0.3 mM, respectively; 3 g of glucose for expression of ^{15}N isotopically labeled TM3/4 V232D. The cells were grown at 37 °C and induced at an O.D. of 0.6 with 0.1 mM IPTG, followed by overnight shaking at room temperature. Harvested cells were sonicated in 20 mM Tris, pH 8.0, and then centrifuged. The soluble fraction was supplemented with NaCl (150 mM), β-mercaptoethanol (20 mM), imidazole (5 mM), and 0.1% Triton X-100, and then applied to a nickel affinity resin (from Qiagen) pre-equilibrated under the same conditions as the protein mixture, and binding was allowed to proceed overnight at room temperature. Elution was performed with the same equilibration buffer containing 400 mM imidazole. Eluted fractions were then treated with $CaCl_2$ (5 mM) and thrombin (15 U). Thrombin-treated TM3/4 V232D was purified by RP-HPLC on a C4 semipreparative column (Phenomenex) using an acetonitrile gradient. Protein-containing fractions were obtained by monitoring A_{215}, and evaporated under nitrogen until they contained less than 20% acetonitrile. The resulting fractions were then lyophilized. The yield was typically *ca.* 18 mg of TM3/4 V232D (>95% pure) per 1 L of minimal M9 medium. The sequence of the TM3/4 construct obtained in this manner is GSGMPDLGTDDDDKAM^{194}GLA LAHFVWIAPLQVALLMGLIWELLQASAFAGLGFLIDLALFQAG-L^{241}GLE HHHHHH, which contains residues 194–241 as numbered in full-length CFTR (TM3/4).

Uniformly ^{15}N labeled Pf1 was prepared as previously described [29], and purified using a previously reported procedure [30].

4.2. Bicelle sample preparation

The uniformly ^{15}N-labeled TM3/4 V232D segment of CFTR and Pf1 major coat protein were reconstituted into bicelles as previously described [31,32]. 1,2-di-*O*-hexyl-sn-glycero-3-phosphocholine (6-*O*-PC) and 1,2-di-*O*-tetradecyl-sn-glycero-3-phosphocholine (14-*O*-PC) were purchased from Avanti Polar Lipids (www.avantilipids.com). About 3–8 mg of lyophilized proteins were dissolved in 9.5 mg of 6-*O*-PC and then the clear solution was added to 45.6 mg of 14-*O*-PC, yielding the protein-containing bicelle samples with a final molar ratio of long chain to short chain lipids (q) of 3.2 and the total lipid concentration of 28% (w/v). A final concentration of 50 mM NaCl and 20 mM Cu–EDTA were added to the CFTR and Pf1 samples, respectively.

4.3. NMR spectroscopy

The NMR experiments were performed on a spectrometer that consisted of a Bruker Avance console interfaced to a Magnex 700/62 mid-bore magnet with a ^{1}H frequency of 699.9 MHz. The ID of the room temperature shims is 48 mm. All samples were equilibrated in the magnetic field at constant temperature for at least 30 min prior to the NMR measurements. The one-dimensional ^{15}N NMR chemical shift spectrum of the CFTR sample was obtained by a 1.0 ms cross polarization with SPINAL-16 [33] ^{1}H decoupling during the 10.2 ms acquisition period using a B_1 radio-frequency strength of 50 kHz. The CFTR sample temperature was regulated at 42 °C. The two-dimensional separated local field SAMPI4 [34] spectrum of Pf1 sample resulted from a total of 48 t_1 increments and 512 t_2 complex points with 64 scans for each t_1 increment. The B_1 radio-frequency strength of 42 kHz and 1.5 s recycle delay with 5 ms acquisition time were used. The sample temperature was regulated at 40 °C. All chemical shifts are referenced externally by setting the ^{15}N resonance of ammonium sulfate to 26.8 ppm at room temperature. NMR spectra were processed using NMRpipe [35].

Acknowledgments

We thank Stanley Howell and Armando Magana for their contributions to the probe development. This research was supported by grants to S.J.O. from the National Institutes of Health and to C.M.D from the Canadian Cystic Fibrosis Foundation; and was performed at the Resource for NMR Molecular Imaging of Proteins, which is supported by Grant P41EB002031.

References

[1] N.I. Avdievich, G.J. Gerfen, Multifrequency probe for pulsed EPR and ENDOR spectroscopy, Journal of Magnetic Resonance 153 (2001) 178–185.
[2] V.R. Cross, R.K. Hester, J.S. Waugh, Single coil probe with transmission-line tuning for nuclear magnetic double-resonance, Review of Scientific Instruments 47 (1976) 1486–1488.
[3] F.D. Doty, R.R. Inners, P.D. Ellis, A multi-nuclear double-tuned probe for applications with solids or liquids utilizing lumped tuning elements, Journal of Magnetic Resonance 43 (1981) 399–416.
[4] Y.J. Jiang, R.J. Pugmire, D.M. Grant, An efficient double-tuned C-13/H-1 probe circuit for CP/MAS NMR and its importance in linewidths, Journal of Magnetic Resonance 71 (1987) 485–494.

[5] R.W. Martin, E.K. Paulson, K.W. Zilm, Design of a triple resonance magic angle sample spinning probe for high field solid state nuclear magnetic resonance, Review of Scientific Instruments 74 (2003) 3045–3061.
[6] J.A. Stringer, G.P. Drobny, Methods for the analysis and design of a solid state nuclear magnetic resonance probe, Review of Scientific Instruments 69 (1998) 3384–3391.
[7] J.B.D. de Lacaillerie, B. Jarry, O. Pascui, D. Reichert, "Cooking the sample": radiofrequency induced heating during solid-state NMR experiments, Solid State Nuclear Magnetic Resonance 28 (2005) 225–232.
[8] S.V. Dvinskikh, V. Castro, D. Sandstrom, Heating caused by radiofrequency irradiation and sample rotation in C-13 magic angle spinning NMR studies of lipid membranes, Magnetic Resonance in Chemistry 42 (2004) 875–881.
[9] C.G. Li, Y.M. Mo, J. Hu, E. Chekmenev, C.L. Tian, F.P. Gao, R.Q. Fu, P. Gor'kov, W. Brey, T.A. Cross, Analysis of RF heating and sample stability in aligned static solid-state NMR spectroscopy, Journal of Magnetic Resonance 180 (2006) 51–57.
[10] C.V. Grant, S.L. Sit, A.A. De Angelis, K.S. Khuong, C.H. Wu, L.A. Plesniak, S.J. Opella, An efficient H-1/P-31 double-resonance solid-state NMR probe that utilizes a scroll coil, Journal of Magnetic Resonance 188 (2007) 279–284.
[11] J.A. Stringer, C.E. Bronnimann, C.G. Mullen, D.H.H. Zhou, S.A. Stellfox, Y. Li, E.H. Williams, C.M. Rienstra, Reduction of RF-induced sample heating with a scroll coil resonator structure for solid-state NMR probes, Journal of Magnetic Resonance 173 (2005) 40–48.
[12] B. Dillmann, K. Elbayed, H. Zeiger, M.C. Weingertner, M. Plotto, F. Engelke, A novel low-E field coil to minimize heating of biological samples in solid-state multinuclear NMR experiments, Journal of Magnetic Resonance 187 (2007) 10–18.
[13] A. Krahn, U. Priller, L. Emsley, F. Engelke, Resonator with reduced sample heating and increased homogeneity for solid-state NMR, Journal of Magnetic Resonance 191 (2008) 78–92.
[14] C.H. Wu, C.V. Grant, G. Cook, S.H. Park, S.J. Opella, A strip shield improves the efficiency of a solenoid coil in probes for high field solid-state NMR of lossy biological samples, Journal of Magnetic Resonance 200 (2009) 74–80.
[15] F.D. Doty, J. Kulkarni, C. Turner, G. Entzminger, A. Bielecki, Using a cross-coil to reduce RF heating by an order of magnitude in triple-resonance multinuclear MAS at high fields, Journal of Magnetic Resonance 182 (2006) 239–253.
[16] P.L. Gor'kov, E.Y. Chekmenev, C.G. Li, M. Cotten, J.J. Buffy, N.J. Traaseth, G. Veglia, W.W. Brey, Using low-E resonators to reduce RF heating in biological samples for static solid-state NMR up to 900 MHz, Journal of Magnetic Resonance 185 (2007) 77–93.
[17] P.L. Gor'kov, R. Witter, E.Y. Chekmenev, F. Nozirov, R. Fu, W.W. Brey, Low-E probe for F-19-H-1 NMR of dilute biological solids, Journal of Magnetic Resonance 189 (2007) 182–189.
[18] S.A. McNeill, P.L. Gor'kov, K. Shetty, W.W. Brey, J.R. Long, A low-E magic angle spinning probe for biological solid state NMR at 750 MHz, Journal of Magnetic Resonance 197 (2009) 135–144.
[19] D.W. Alderman, D.M. Grant, Efficient decoupler coil design which reduces heating in conductive samples in superconducting spectrometers, Journal of Magnetic Resonance 36 (1979) 447–451.
[20] Z. Zhang, P.C. Hammel, G.J. Moore, Application of a novel RF coil design to the magnetic resonance force microscope, Review of Scientific Instruments 67 (1996) 3307–3309.
[21] E.K. Paulson, R.W. Martin, K.W. Zilm, Cross polarization, radio frequency field homogeneity, and circuit balancing in high field solid state NMR probes, Journal of Magnetic Resonance 171 (2004) 314–323.
[22] C.S. Zuo, K.R. Metz, Y. Sun, A.D. Sherry, NMR temperature measurements using a paramagnetic lanthanide complex, Journal of Magnetic Resonance 133 (1998) 53–60.
[23] D.G. Gadian, F.N.H. Robinson, Radiofrequency losses in NMR experiments on electrically conducting samples, Journal of Magnetic Resonance 34 (1979) 449–455.
[24] R. Linser, V. Chevelkov, A. Diehl, B. Reif, Sensitivity enhancement using paramagnetic relaxation in MAS solid-state NMR of perdeuterated proteins, Journal of Magnetic Resonance 189 (2007) 209–216.
[25] N.P. Wickramasinghe, M. Kotecha, A. Samoson, J. Past, Y. Ishii, Sensitivity enhancement in C-13 solid-state NMR of protein microcrystals by use of paramagnetic metal ions for optimizing H-1 T-1 relaxation, Journal of Magnetic Resonance 184 (2007) 350–356.
[26] A. Rath, M. Glibowicka, V.G. Nadeau, G. Chen, C.M. Deber, Detergent binding explains anomalous SDS–PAGE migration of membrane proteins, Proceedings of the National Academy of Sciences of the United States of America 106 (2009) 1760–1765.
[27] A.G. Therien, M. Glibowicka, C.M. Deber, Expression and purification of two hydrophobic double-spanning membrane proteins derived from the cystic fibrosis transmembrane conductance regulator, Protein Expression and Purification 25 (2002) 81–86.
[28] H. Wehbi, G. Gasmi-SeabrooK, M.Y. Choi, C.M. Deber, Positional dependence of non-native polar mutations on folding of CFTR helical hairpins, Biochimica et Biophysica Acta – Biomembranes 1778 (2008) 79–87.
[29] D.S. Thiriot, A.A. Nevzorov, L. Zagyanskiy, C.H. Wu, S.J. Opella, Structure of the coat protein in Pf1 bacteriophage determined by solid-state NMR Spectroscopy, Journal of Molecular Biology 341 (2004) 869–879.
[30] S.H. Park, C. Loudet, F.M. Marassi, E.J. Dufourc, S.J. Opella, Solid-state NMR spectroscopy of a membrane protein in biphenyl phospholipid bicelles with the bilayer normal parallel to the magnetic field, Journal of Magnetic Resonance 193 (2008) 133–138.
[31] A.A. De Angelis, A.A. Nevzorov, S.H. Park, S.C. Howell, A.A. Mrse, S.J. Opella, High-resolution NMR spectroscopy of membrane proteins in aligned bicelles, Journal of the American Chemical Society 126 (2004) 15340–15341.
[32] A.A. De Angelis, S.J. Opella, Bicelle samples for solid-state NMR of membrane proteins, Nature Protocols 2 (2007) 2332–2338.
[33] B.M. Fung, A.K. Khitrin, K. Ermolaev, An improved broadband decoupling sequence for liquid crystals and solids, Journal of Magnetic Resonance 142 (2000) 97–101.
[34] A.A. Nevzorov, S.J. Opella, Selective averaging for high-resolution solid-state NMR spectroscopy of aligned samples, Journal of Magnetic Resonance 185 (2007) 59–70.
[35] F. Delaglio, S. Grzesiek, G.W. Vuister, G. Zhu, J. Pfeifer, A. Bax, NMRpipe – a multidimensional spectral processing system based on unix pipes, Journal of Biomolecular NMR 6 (1995) 277–293.